The peroxin PEX14 of Neurospora crassa is essential for the biogenesis of both glyoxysomes and Woronin bodies

Managadze, David; Wuertz, Christian; Sichting, Martin; Niehaus, Gerd; Veenhuis, Marten; Rottensteiner, Hanspeter; Würtz, Christian

Published in:
Traffic

DOI:
10.1111/j.1600-0854.2007.00560.x

Publication date:
2007

Traffic 2007; **8:** 687–701
Blackwell Munksgaard

doi: 10.1111/j.1600-0854.2007.00560.x

The Peroxin PEX14 of *Neurospora crassa* is Essential for the Biogenesis of Both Glyoxysomes and Woronin Bodies

David Managadze[1,†], Christian Würtz[1,†], Martin Sichting[2,3], Gerd Niehaus[1], Marten Veenhuis[4] and Hanspeter Rottensteiner[1,*]

[1]*Institut für Physiologische Chemie, Abt. Systembiochemie, Ruhr-Universität Bochum, 44780 Bochum, Germany*
[2]*Fachbereich Biologie, Chemie, Pharmazie, Freie Universität Berlin, 14195 Berlin, Germany*
[3]*Current address: Lehrstuhl für Physiologische Chemie, Ludwig-Maximilian-Universität München, 81377 München, Germany*
[4]*Institute of Biology, University of Groningen, Department of Eukaryotic Microbiology, 9751 NN Haren, The Netherlands*
**Corresponding author: Hanspeter Rottensteiner, hanspeter.rottensteiner@rub.de*
†*These authors contributed equally to the manuscript.*

In the filamentous fungus *Neurospora crassa*, glyoxysomes and Woronin bodies coexist in the same cell. Because several glyoxysomal matrix proteins and also HEX1, the dominant protein of Woronin bodies, possess typical peroxisomal targeting signals, the question arises as to how protein targeting to these distinct yet related types of microbodies is achieved. Here we analyzed the function of the *Neurospora* ortholog of PEX14, an essential component of the peroxisomal import machinery. PEX14 interacted with both targeting signal receptors and was localized to glyoxysomes but was virtually absent from Woronin bodies. Nonetheless, a *pex14Δ* mutant not only failed to grow on fatty acids because of a defect in glyoxysomal β-oxidation but also suffered from cytoplasmic bleeding, indicative of a defect in Woronin body-dependent septal pore plugging. Inspection of *pex14Δ* mutant hyphae by fluorescence and electron microscopy indeed revealed the absence of Woronin bodies. When these cells were subjected to subcellular fractionation, HEX1 was completely mislocalized to the cytosol. Expression of GFP-HEX1 in wild-type mycelia caused the staining of Woronin bodies and also of glyoxysomes in a targeting signal-dependent manner. Our data support the view that Woronin bodies emerge from glyoxysomes through import of HEX1 and subsequent fission.

Key words: filamentous fungus, HEX1, peroxisomal targeting signal, peroxisome, protein translocation, *Saccharomyces cerevisiae*

Received 28 September 2006, revised and accepted for publication 23 February 2007, published online 25 April 2007

Microbodies comprise a number of multipurpose organelles with essential functions including peroxisomes, glyoxysomes, glycosomes and Woronin bodies (1,2). Depending on organism, cell type and metabolic need, distinct sets of proteins are housed within microbodies. Peroxisomes and glyoxysomes typically contain a complete fatty acid β-oxidation system, with glyoxysomes additionally harboring the key enzymes of the glyoxylate cycle, isocitrate lyase and malate synthase (3). Glycosomes of the trypanosomes are typified by the presence of enzymes engaged in glycolysis, which is a compartmentalized process in these species (4,5). Woronin bodies are a characteristic of filamentous fungi; they encompass hexagonal crystals of HEX1, the dominant protein of this organelle (6). One established function of Woronin bodies is the plugging of the septal pores after hyphal wounding, which restricts the loss of cytoplasm to the sites of injury (7–9). A *hex1* mutant is more vulnerable, as cytoplasm streams out also from neighboring, intact segments because of the lack of hyphal sealing. This bleeding becomes manifest in yellowish droplets, particularly when grown on solid media promoting hyphal branching.

A single organism may house different types of microbodies. During the development of plants, for instance, germination of seedlings initially requires glyoxysomes to degrade storage lipids via β-oxidation. Later on, glyoxysomes are transformed into peroxisomes through a change in the expression pattern so as to adapt the matrix enzyme content to the need for photorespiration. In senescing tissue, glyoxysomes are again formed out of peroxisomes (10). While the described transformation is controlled in a temporal manner, *Neurospora crassa* and several other filamentous ascomycetes are unique in that they usually possess two distinct types of microbodies within a single cell at the same time, glyoxysomes and Woronin bodies (11,12).

Despite the differences in function, microbodies possess basically conserved protein-import machineries. Proteins destined to microbodies usually possess a peroxisomal targeting signal type 1 (PTS1) at the extreme C-terminus that is composed of the tripeptide SKL or conservative variants thereof (13,14). A few proteins such as 3-ketoacyl-CoA thiolase are targeted via a more N-terminal PTS2 signal (15), and some others possess neither of the two signals (16,17). The import of matrix proteins is governed by a set of proteins called peroxins. The soluble import receptor for PTS1 proteins, PEX5, recognizes cargo proteins

in the cytosol and delivers them to the docking complex at the peroxisomal membrane, with its central components PEX13 and PEX14. Following docking, cargo protein is translocated via an unknown mechanism. The unloaded PEX5 is then thought to shuttle back to the cytosol, enabled by the participation of a number of additional peroxins (for recent reviews, see 18–22). The PTS2 receptor PEX7 is likely to run through a similar cycle with the exception that it additionally depends on a species-specific auxiliary factor or coreceptor, such as PEX20 in *N. crassa* and several other fungi (23–26). Import of proteins that possess neither a PTS1 nor a PTS2 depended on PEX5 in all cases analyzed, albeit here a distinct domain of PEX5 is used for cargo recognition (16,17,27).

This work concerns the differential protein import into glyoxysomes and Woronin bodies in *N. crassa*. Because both types of organelles harbor matrix proteins with canonical peroxisomal targeting signals (HEX1 ends with SRL; 7,8), their formation and maintenance requires mechanisms to ensure that resident proteins are sorted to the correct organelle. Considering that the *N. crassa* genome encodes only a single set of peroxins (23,28), selective targeting of HEX1 to Woronin bodies might be achieved by (i) a Woronin body-specific import apparatus that is unrelated to the typical peroxin machinery, (ii) a peroxin import machinery that is also localized to Woronin bodies but additionally equipped with selectivity factors or (iii) an import into glyoxysomes and a subsequent fission of Woronin bodies from glyoxysomes. The last mechanism is supported by early electron micrographs (29), as well as by recent data showing a transient colocalization of Woronin bodies and GFP-SKL (30). However, direct evidence for a common import route of HEX1 and glyoxysomal matrix proteins is still lacking.

Here we characterized the PEX14 ortholog of *N. crassa* and determined its role in the biogenesis of glyoxysomes and Woronin bodies by various cell biological and biochemical approaches. The results are discussed in terms of a model in which the glyoxysome is the sole site of protein import from which Woronin bodies emerge through fission.

Results

Identification and isolation of the N. crassa orthologs of pex13 and pex14

To study the role of peroxins in the differential protein import into glyoxysomes and Woronin bodies, the putative *Neurospora* orthologs of PEX13 and PEX14 were selected for functional analysis. These two proteins proved essential for peroxisomal matrix protein import in all species studied so far and possess a defined role as integral constituents of the peroxisomal docking complex. According to the annotated *N. crassa* genome at the Broad Institute assembly 7 (31), the *pex13* gene refers to locus NCU02618.3 and *pex14* to NCU03901.3. Both reading frames are predicted to contain two introns. Amplification of *pex13* and *pex14* with specific primer pairs from genomic DNA as well as from a cDNA library confirmed the published genome sequence as well as the number and positions of the predicted introns (*pex13*—intron I: bp 56–132, intron II: bp 664–729; *pex14*—intron I: bp 41–120, intron II: bp 447–502). The deduced amino acid sequences of PEX13 and PEX14 were aligned with the orthologs from *Saccharomyces cerevisiae* and *Pichia pastoris* using CLUSTALW (32). PEX13 showed two regions with strong conservation: the C-terminal SH3 domain, required for the interaction with PEX14 and PEX5, and amino acids 164–221, which include at least one transmembrane domain (Figure S1). As in all PEX13 proteins, the N-terminus of PEX13 is rich in glycine residues, but the significance of this feature is unclear. PEX14 also showed a significant degree of similarity with the yeast orthologs, particularly at its N-terminus that usually binds PEX5 (Figure S2).

PEX13 and PEX14 interact with both PTS receptors and with each other

To obtain experimental evidence for a role of the two novel *N. crassa* proteins in docking, PEX13 and PEX14 were tested in a two-hybrid assay for interaction with the import receptors. PEX14 strongly interacted with the soluble PTS2 receptor PEX7 (23) and weakly with the PEX7-associated PEX20 (Figure 1A). As observed in *S. cerevisiae* and mammals (33–35), PEX13 also interacted with PEX7 and its SH3 domain showed binding toward PEX20 (Figure 1B). The endogenous PTS1 import receptor PEX5 remains to be cloned, but interactions of PEX14 and PEX13 were detected with PEX5 from *S. cerevisiae* (Figure 1A,B). The two-hybrid data therefore suggested that both *Neurospora* proteins are able to bind the PTS1 and PTS2 import receptors and indeed represent the *N. crassa* orthologs of PEX13 and PEX14.

PEX14 is also known to interact with the SH3 domain of PEX13 (36–38). Because this interaction was only passably emulated by the *Neurospora* orthologs in the two-hybrid system (Figure 1C), a complementary approach was additionally used. A hexahistidine-tagged version of PEX14 was overexpressed in *N. crassa* and isolated from detergent-solubilized membranes by affinity chromatography. The presence of PEX13 and PEX14 in the respective samples was then analyzed by immunoblotting using specific antibodies that had been generated against the recombinant proteins (Figure S3). A significant fraction of PEX13 coeluted with His_6-PEX14 (Figure 2). This was not the case for the mitochondrial membrane protein TIM23 and the dominant Woronin body protein HEX1. Furthermore, PEX13 did not elute when solubilized wild-type membranes were applied to the column (Figure 2). Thus, binding of PEX13 to PEX14 appeared specific, consistent with previous reports showing that a fraction of PEX13 associated with purified PEX14 from mammals (38–40) and yeast (41,42).

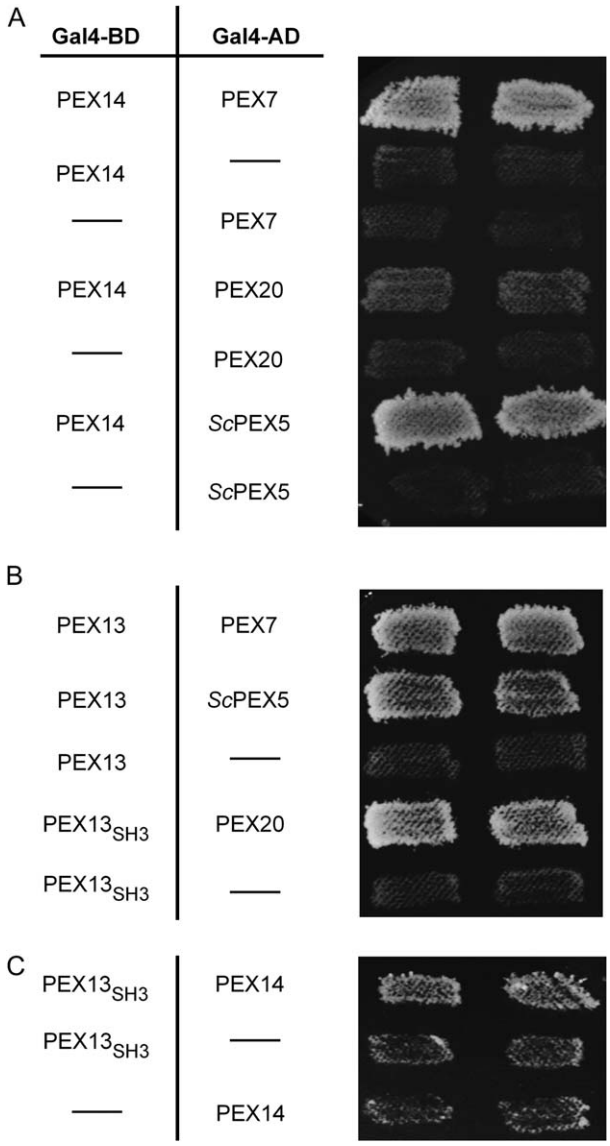

Figure 1: Interactions of *Neurospora crassa* PEX13 and PEX14 with PTS import receptors by yeast two-hybrid analysis. A) Analysis of PEX14 interactions. PEX14 was fused to the *GAL4*-binding domain (Gal4-BD) and tested for interaction with *GAL4*-activation domain (Gal4-AD) fusions of PEX7, PEX20 and *Saccharomyces cerevisiae* PEX5 (*Sc*PEX5). The indicated plasmid combinations were cotransformed into the two-hybrid strain PJ69-4a, with empty pPC86 (Gal4-AD) or pPC97 (Gal4-BD) serving as negative control. Two independent transformants were tested for prototrophy on histidine adenine double-dropout plates. B) Analysis of interactions of PEX13 or its SH3 domain. The respective *GAL4*-binding domain fusions were similarly tested for interaction with the import receptors. C) Test for interaction of PEX14 with the SH3 domain of PEX13.

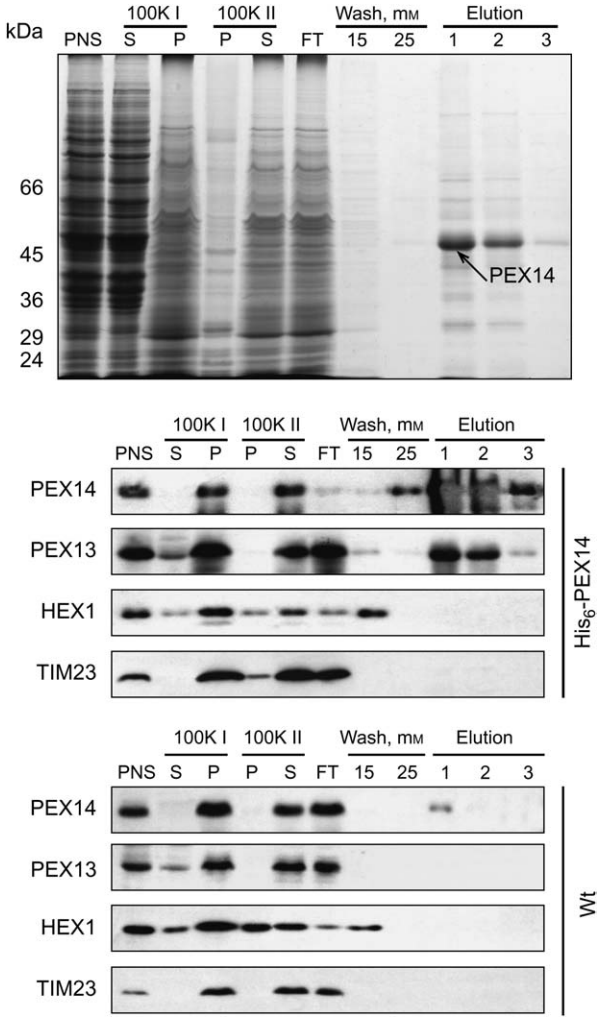

Figure 2: Association of PEX13 with PEX14. A *Neurospora crassa* wild-type strain expressing a His_6-tagged variant of PEX14 was analyzed for the presence of PEX13 in the eluate of His_6-PEX14 that had been selectively enriched through a Ni-NTA column. The top panel shows a Coomassie-stained gel of the purification. In the middle panel, proteins were identified via immunoblotting using antisera against PEX14, PEX13, HEX1, and TIM23. For the immunological detection of His_6-PEX14, samples were diluted 10-fold. A fraction of PEX13 selectively coeluted with His_6-PEX14. The bottom panel shows the immunological analysis of the control purification using wild-type extract (Wt). The eluate was devoid of PEX13. Note that a small amount of native PEX14 was retained on the Ni-NTA column, likely through unspecific interaction. PNS, post-nuclear supernatant; 100K I, 100 000 × ***g*** centrifugation of the PNS; 100K II, 100 000 × ***g*** centrifugation after solubilization of the 100K I pellet with 1% digitonin; S, supernatant; P, pellet; FT, flow through; Wash, washing buffer containing 15 mM or 25 mM imidazol; Elution (with three 2-ml fractions), elution buffer containing 150 mM imidazol.

PEX13 and PEX14 are localized to glyoxysomes

To determine the subcellular localization of the two *N. crassa* peroxins, a post-nuclear supernatant (PNS) obtained from an *N. crassa* wild-type strain was subjected to differential centrifugation at 27 000 × ***g*** to sediment heavy organelles including mitochondria and glyoxysomes, followed by a 200 000 × ***g*** centrifugation step to sediment light vesicles, particularly the microsomal fraction. As expected, the inner mitochondrial membrane marker

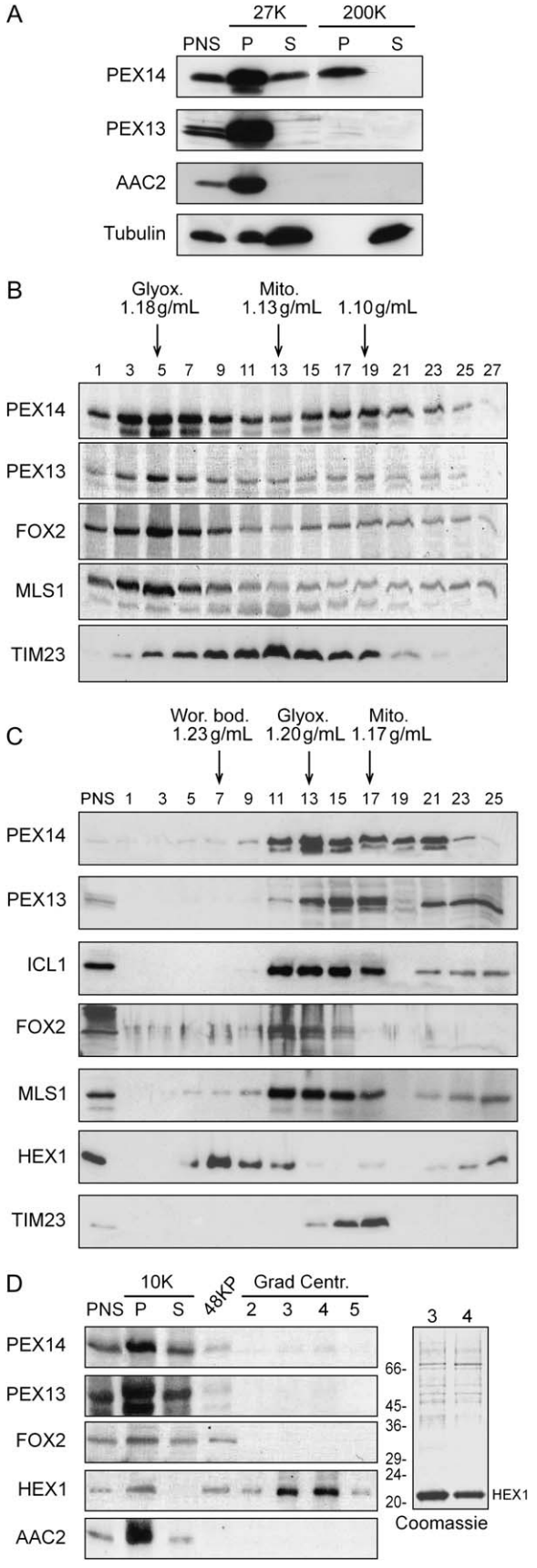

protein AAC2 was recovered exclusively in the 27 000 × ***g*** organellar pellet, and the majority of the cytosolic tubulin was detected in the 200 000 × ***g*** supernatant fraction (Figure 3A). PEX14 was predominantly observed in the 27 000 × ***g*** pellet but also in the 200 000 × ***g*** pellet fraction, whereas PEX13 was only recovered from the 27 000 × ***g*** pellet fraction. This result indicated that PEX13 and PEX14 are indeed localized to membrane-bound structures; it further suggested that PEX14 is additionally present in lower density vesicles.

To pursue this in more detail, the distribution of PEX13 and PEX14 was analyzed in a Nycodenz gradient that allows a clear separation of mitochondria from glyoxysomes. For this, a PNS from oleic acid-induced *N. crassa* wild-type hyphae was loaded on such a gradient (10–35%, w/v) and separated by centrifugation. PEX14 entered the gradient with its peak fraction at a density of 1.18 g/mL (Figure 3B). The mitochondrial marker protein TIM23 showed a distinct distribution (peak fraction at 1.13 g/mL), indicating that

Figure 3: Subcellular localization of PEX13 and PEX14. A) Differential centrifugation. A PNS from *Neurospora crassa* wild-type mycelia was separated by consecutive centrifugation at 27 000 × ***g*** (27K) and 200 000 × ***g*** (200K). In all, 50 μg of the resulting pellet (P) and supernatant (S) fractions were loaded on a gel and subjected to Western blot analysis. The distribution of PEX14, PEX13, mitochondrial AAC2 and cytosolic tubulin was determined with appropriate antibodies. B) Nycodenz density gradient centrifugation. A PNS from oleic acid-induced *N. crassa* wild-type mycelia was loaded on top of a linear Nycodenz density gradient (10–35%, w/v) and subjected to centrifugation at 40 000 × ***g*** for 2 h. Fractions were collected from the bottom (fraction 1) to the top and were assayed by Western blot for the distribution of PEX14, PEX13 and glyoxysomal (multifunctional β-oxidation enzyme FOX2 and malate synthase MLS1) and mitochondrial (TIM23) marker enzymes. The densities of the peak glyoxysomal (Glyox.) and mitochondrial (Mito.) fractions, as well as that of an additional PEX14 peak appearing at lighter fractions, are indicated. C) Sucrose density gradient centrifugation. A PNS of oleic acid-induced *N. crassa* wild-type mycelia was subjected to 30–60% (w/w) sucrose density gradient centrifugation at 40 000 × ***g*** for 2 h. One-milliliter fractions were collected from the bottom (fraction 1) to the top and analyzed for the distribution of PEX14, PEX13, the glyoxysomal markers isocitrate lyase ICL1, MLS1 and FOX2, as well as the Woronin body marker protein HEX1. TIM23 served as mitochondrial marker. The densities of the peak fractions of Woronin bodies (Wor. bod.), glyoxysomes and mitochondria are indicated. D) Woronin body purification. A heavy organelle fraction (10K) obtained from a PNS of sucrose-grown wild-type mycelia was resuspended, layered on top of a 52% sucrose cushion and subjected to density barrier centrifugation at 48 000 × ***g*** for 1 h. The resulting Woronin body-enriched pellet (48KP) was again resuspended and subjected to sucrose density gradient centrifugation as described under (C). Shown are the gradient fractions 2–5 (Grad Centr.), with HEX1 being concentrated in fractions 3 and 4. These fractions were devoid of the mitochondrial ATP/ADP carrier AAC2 and glyoxysomal FOX2 and PEX13, and contained only minute amounts of PEX14. Proteins present in fractions 3 and 4 were also visualized by Coomassie staining.

PEX14 was not localized to mitochondria. Rather, PEX14 cosedimented with the glyoxysomal marker proteins malate synthase (MLS1) and the multifunctional enzyme (FOX2). Similar results were obtained for PEX13. While this congruent distribution demonstrated that PEX13 and PEX14 localize to glyoxysomes, a second peak at lighter densities (1.10 g/mL) was noted for PEX14 and FOX2. Because of the appearance of glyoxysomes almost at the very end of the gradient, the Woronin bodies did not separate well from glyoxysomes in Nycodenz gradients even though they are significantly denser. For their separation, a sucrose density gradient (30–60%, w/w) was performed. Mitochondrial TIM23 peaked at a density of 1.17 g/mL and the glyoxysomal marker proteins MLS1, ICL1 and FOX2 were all detected at the expected density of mature glyoxysomes (1.20 g/mL) and to varying extents also in lighter fractions (Figure 3C). The dominant Woronin body protein HEX1 was detected at a peak density of 1.23 g/mL, demonstrating that these organelles were clearly separated from glyoxysomes. As expected already from the distribution of PEX14 in the Nycodenz gradient, a significant portion of PEX14 cosedimented with the glyoxysomal marker proteins and the rest was recovered from lighter fractions. PEX13 was also present in the glyoxysomal fractions, albeit a shift in the peak density to lighter fraction was noted. Remarkably, the peak Woronin body fraction was apparently devoid of PEX13 and PEX14.

To corroborate this, Woronin bodies were enriched by a multistep procedure. A 10 000 $\times$ ***g*** pellet fraction of a PNS from sucrose-grown wild-type hyphae was resuspended and subjected to sedimentation through a dense sucrose cushion to remove the majority of glyoxysomes and mitochondria. The pellet was resuspended, and the Woronin bodies contained in this pellet were further purified by sucrose density gradient centrifugation. The immunoblots in Figure 3D show the selective enrichment of Woronin bodies: HEX1 was recovered from gradient fractions 3 and 4, while mitochondrial AAC2, glyoxysomal FOX2 and PEX13 were virtually absent in these samples. The very weak signal obtained for PEX14 indicated that minute amounts of this peroxin were present in Woronin bodies but at the same time suggested that PEX14 is dispensable for the function of mature Woronin bodies. This observation raised the question whether the import of HEX1 into Woronin bodies is at all dependent on PEX14.

A pex14 deletion strain exhibits microbody-specific defects

The role of PEX14 in the biogenesis of glyoxysomes and Woronin bodies was analyzed by using a *pex14* knockout strain. The strain exhibited clear macroscopic abnormalities. When grown on solid Vogel's minimal medium (VMM) containing 2% sucrose, yellow to orange-colored droplets appeared, indicative of a substantial loss of cytoplasm and reminiscent of the phenotype of a *hex1*^{RIP} mutant. A direct comparison of the two mutants revealed that egression of cytoplasm was more pronounced for the *pex14Δ* strain (Figure 4A). Another striking feature of the *pex14Δ* mutant was its inability to form macroconidia from aerial hyphae.

A defect in the biogenesis of microbodies should result in an inability to degrade fatty acids because long-chain fatty acids are thought to be exclusively degraded within glyoxysomes of *N. crassa* (3). Indeed, *pex14Δ* hyphae failed to grow in the presence of oleic acid, whereas the *hex1*^{RIP} mutant grew well (Figure 4B,C). The latter strain also exhibited a morphological phenotype on these plates. In contrast to the wild-type colony, which formed periodic zones of conidiated hyphae as a consequence of its circadian clock (43,44), the *hex1*^{RIP} mutant grew as a continuous and flat mycelium (Figure 4B). Tergitol NP-40, the detergent used to solubilize the fatty acid, allowed some flimsy growth of all strains tested (not shown), indicating not only that the *pex14Δ* mutant was unable to use oleic acid but also that the fatty acids actively inhibited growth.

The specificity of this growth defect was further supported by the ability of the *pex14Δ* mutant to grow on the nonfermentable C_2-carbon source ethanol (Figure 4C). Finally, despite strong differences in mycelia densities, growth rates of the mutant strains were comparable to that of the wild type on solid sucrose-containing VMM (Figure 4C). In summary, the observed phenotype of the mutant, particularly bleeding and an inability to use fatty acids, was in agreement with a function of PEX14 in the biogenesis of both Woronin bodies and glyoxysomes.

The peroxin PEX2 (previously dubbed PAF1) was reported to be essential for sexual development of the filamentous ascomycete *Podospora anserina* (45). To test whether this is also the case in *N. crassa*, strains of opposite mating type but homozygous for the *pex14Δ* deletion were crossed and inspected for the formation of perithecia. Fruiting bodies did not emerge from the cross, whereas in the wild-type control, macroscopic, discernible, black spots representing perithecia were abundant (Figure 4D). Crossing the mutant with the wild-type strain further revealed that *pex14Δ* strains are fertile as male parents, but are female sterile. These observations demonstrated that microbodies are important for sexual development in *N. crassa*.

Woronin bodies are absent in pex14Δ hyphae

The ultrastructure of *N. crassa* hyphae was examined for the appearance of hexagonal Woronin bodies. In oleic acid-induced wild-type hyphae, both glyoxysomes and electron-dense hexagonal structures typified as Woronin bodies were discernible (Figure 5A). Occasionally, a Woronin body was found within the septal pore (Figure 5B). Immunogold labeling with the anti-HEX1 antibody demonstrated that HEX1 is located within Woronin bodies (Figure 5C),

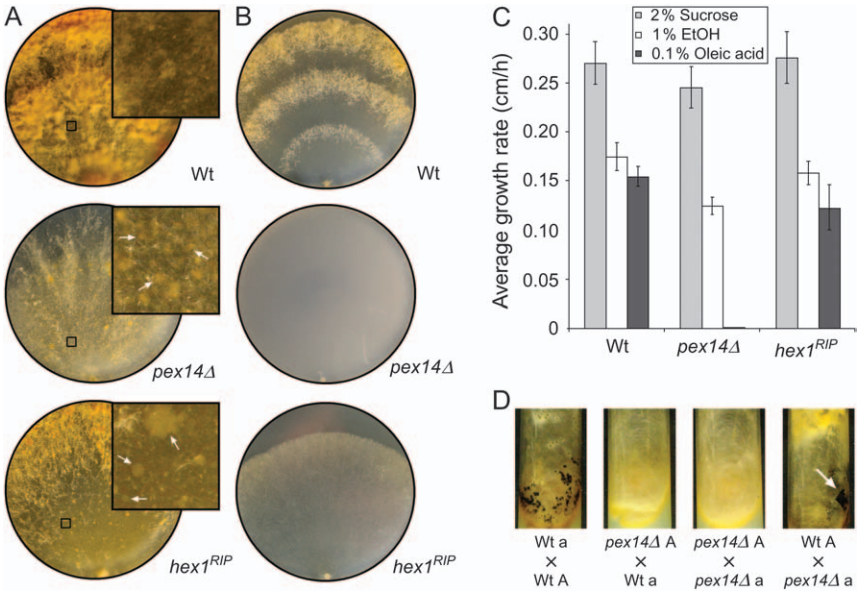

Figure 4: Effect of a *pex14Δ* deletion on Woronin body and glyoxysomal functions. A) Loss of cytoplasm upon growth on solid agar medium. A small piece of agar with mycelia from a wild-type strain, the *pex14Δ* mutant or the Woronin body mutant *hex1*^{RIP} was transferred to the edge of a new plate composed of VMM supplemented with 2% sucrose. Prior to recording, plates were incubated at 30°C for 4 days. Insets show a 12-fold magnification of the marked sections of the plates. Arrows denote liquid droplets, representing cytoplasm that had streamed out of damaged hyphae. B, C) Test for growth on fatty acids as sole carbon source. Mycelia from the same strains were applied to sucrose-, ethanol-, or oleic acid-containing VMM plates as described in (A) and incubated for 4 days at 30°C. Shown are (B) the oleic acid plates after 4 days and (C) the determined average growth rates (cm/h). The *pex14Δ* strain was specifically impaired for growth on oleic acid. D) Formation of perithecia. For crossing, the female partner strains (upper line) were grown in test tubes on synthetic crossing medium for 4 days. Subsequently, mycelium of the male partner (lower line) was added on a small piece of agar and the tubes were incubated until perithecia became visible for the wild-type cross. The arrow denotes perithecia covering the agar slice.

whereas glyoxysomes remained unstained. By contrast, anti-FOX2 antibodies recognized the multifunctional enzyme exclusively in glyoxysomes (Figure 5D), thereby demonstrating that there is virtually no overlap in the targeting of cargo proteins to the two related organelles.

Because the *pex14Δ* strain did not survive the incubation on oleic acid, its ultrastructure was determined from ethanol-grown cells. As control, the *hex1*^{RIP} strain lacking functional Woronin bodies was also analyzed. Most importantly, hyphae of neither strain possessed hexagonal Woronin bodies (Figure 5E–H). Notably, in both mutant strains electron-dense material was clearly discernible around some of the septal pores (Figure 5G,H). This material is likely to represent deposition plugs able to occlude septa in a Woronin body-independent manner in older, yet intact, hyphae (46). Finally, typical glyoxysomes were also absent from the *pex14Δ* mutant (Figure 5E,G), whereas they did appear in the *hex1*^{RIP} mutant (Figure 5F,H). The micrographs thus supported the view that PEX14 controls the biogenesis of both Woronin bodies and glyoxysomes.

Mislocalization of matrix proteins from Woronin bodies and glyoxysomes in pex14Δ cells

To determine the distribution of organellar marker proteins in the *pex14Δ* strain, PNS was prepared from hyphae grown on sucrose, where *pex14Δ* cells are viable and subjected to differential centrifugation. To preferentially sediment Woronin bodies at lower speed, 5000, 10 000, 25 000 and 100 000 × ***g*** centrifugation steps were used. From the wild-type extract, HEX1 was recovered predominantly in the 5000 and 10 000 pellet fractions, whereas ICL1, MLS1 and FOX2 were distributed between various pellets, probably reflecting glyoxysomal populations of varying densities (Figure 6A). In an extract obtained from the *pex14Δ* strain, HEX1 and MLS1 were exclusively found in the supernatant (Figure 6B). By contrast, ICL1 and FOX2 were additionally detected in the 25 000 and 100 000 pellet fractions. To substantiate the observed protein import defect, PNS prepared from sucrose-grown wild-type or *pex14Δ* hyphae was subjected to density gradient centrifugation. Both strains showed a comparable distribution of mitochondrial TIM23 (Figure 6C,D). HEX1 peaked at a density typical for Woronin bodies in the wild-type strain but was found exclusively in the upper fractions representing cytosol in the *pex14Δ* mutant. In the latter strain, the glyoxysomal MLS1 also did not enter the gradient, whereas a significant portion of ICL1 was present in denser fractions.

The observed import defect for HEX1 was also analyzed by a protease protection assay. For this, PNS prepared from

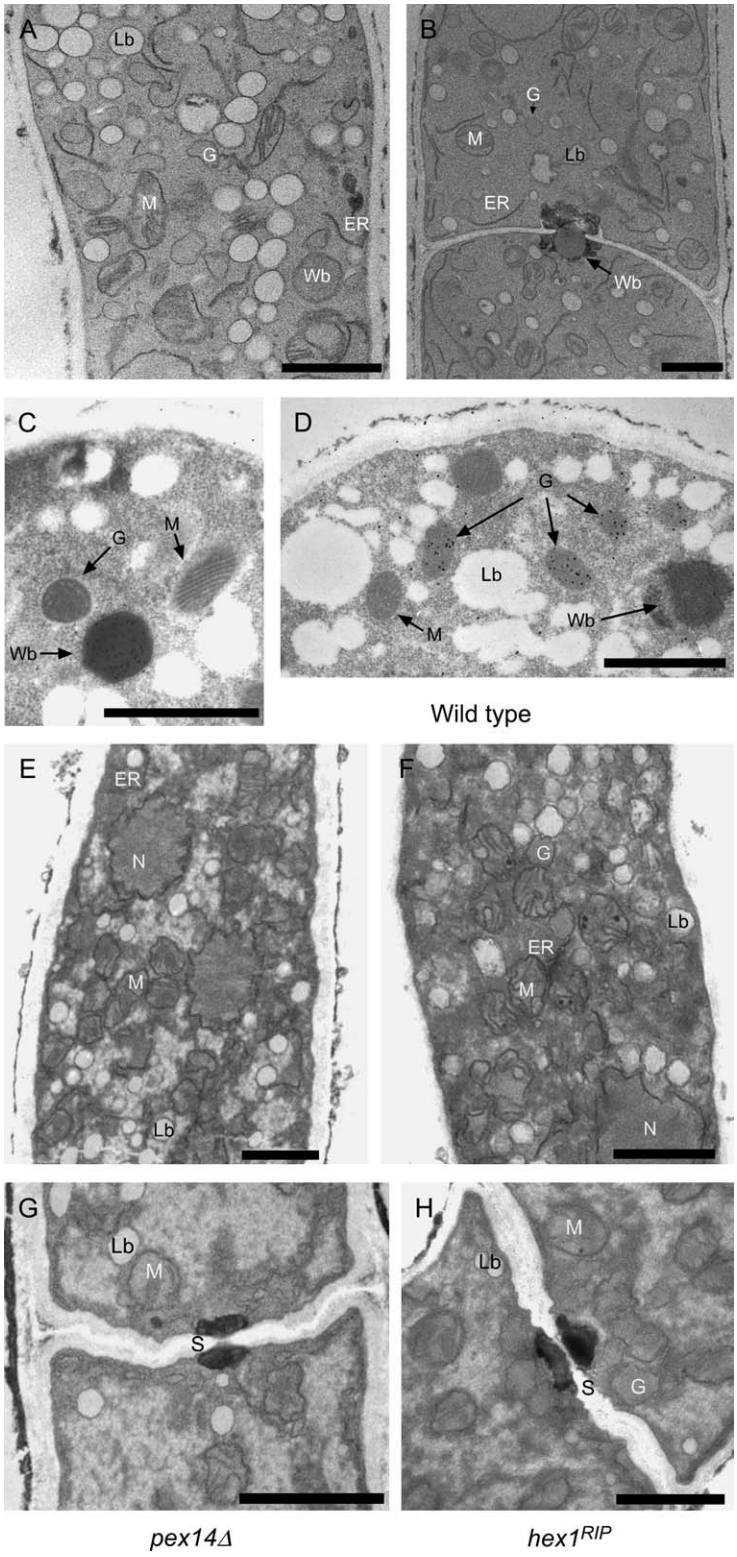

Figure 5: Ultrastructure of Woronin bodies and glyoxysomes and the role of PEX14 in their biogenesis. Mycelia of a wild-type (A–D), a *pex14Δ* (E, G) and a *hex1*^{RIP} (F, H) mutant strain were grown in medium containing oleic acid (A–D) or ethanol (E–H) as sole carbon source and processed for electron microscopy. A) Typical morphology of a wild-type cell. B) A Woronin body plugging the septal pore. C, D) Specific, mutually exclusive staining of Woronin bodies and glyoxysomes with anti-HEX1 (C) and anti-FOX2 (D) antibodies, used in combination with gold-conjugated goat anti-rabbit antiserum. E–H) Absence of Woronin bodies from *pex14Δ* (E, G) and *hex1*^{RIP} (F, H) mutants. E, G) Absence of mature glyoxysomes from the *pex14Δ* mutant. G, H) Woronin body-independent appearance of electron-dense material in septal pores. ER, endoplasmic reticulum; G, glyoxysome; Lb, lipid body; M, mitochondria; N, nucleus; S, septum; Wb, Woronin body. Bar = 1 μm.

the wild-type and the *pex14Δ* mutant were treated with proteinase K, either in the absence or in the presence of detergent. In the wild-type extract, HEX1 and glyoxysomal FOX2 were protected from the protease but not when the integrity of the membranes was destroyed by Triton-X-100, indicating that the analyzed proteins were localized in a membrane-bound compartment (Figure 6E). In case of the *pex14Δ* extract, HEX1 was degraded even without

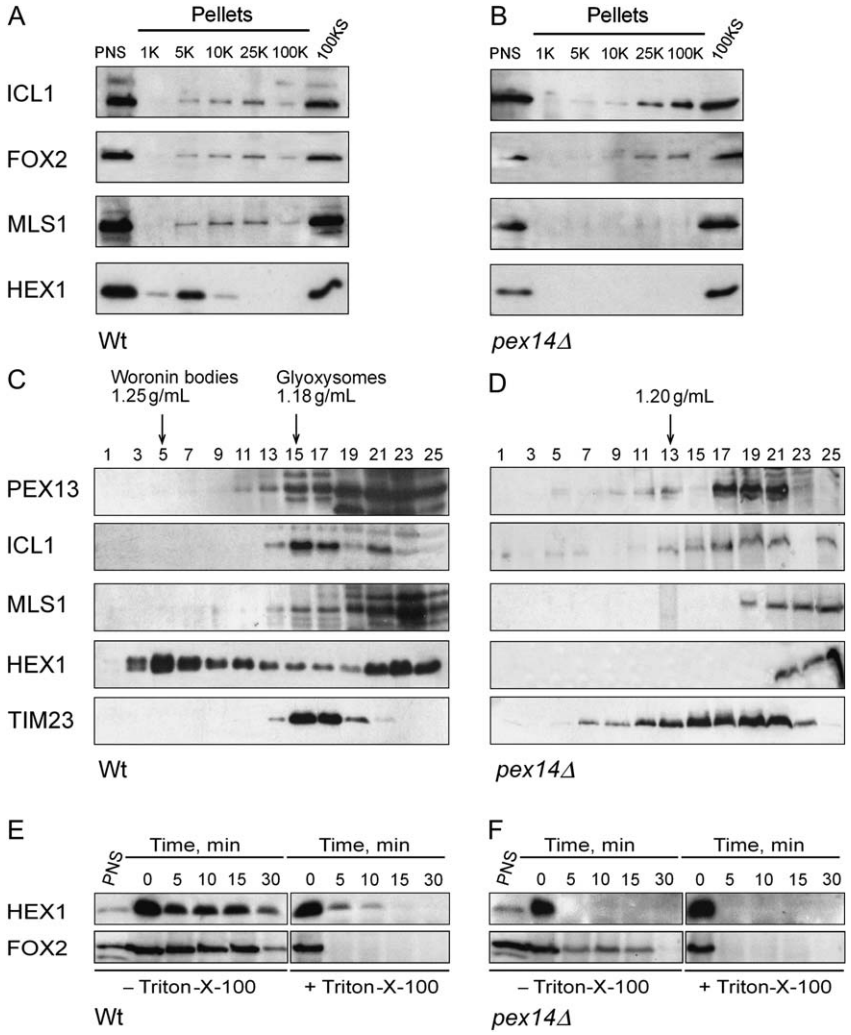

Figure 6: Subcellular distribution of matrix proteins in a *pex14Δ* mutant. A, B) Differential centrifugation. PNS obtained from sucrose-grown mycelia of a wild-type (A) and *pex14Δ* (B) strain were subjected to differential centrifugation at 1000 × ***g*** (1K), 5000 × ***g*** (5K), 10 000 × ***g*** (10K), 25 000 × ***g*** (25K) and 100 000 × ***g*** (100K). Equal portions of each pellet and the final 100 000 × ***g*** supernatant (100KS) were processed for Western blot analysis. Appropriate antibodies were applied to determine the distribution of HEX1, MLS1, ICL1 and FOX2. C, D) Sucrose density gradient centrifugation. Extracts from a wild-type (C) and *pex14Δ* (D) strain grown on sucrose as sole carbon source were loaded on top of a 30–60% (w/w) sucrose density gradient and subjected to centrifugation at 40 000 × ***g*** for 2 h. One-milliliter fractions were collected from the bottom (fraction 1) to the top and analyzed for the distribution of HEX1, glyoxysomal MLS1 and ICL1 as well as mitochondrial TIM23. The densities of peak fractions, indicated by arrows, are also denoted. The PTS1 proteins HEX1 and MLS1 were mislocalized to the cytosol in the *pex14Δ* mutant. E, F) Protease protection assay. PNS of wild-type (E) and *pex14Δ* (F) strain were treated with 100 μg/mL proteinase K and incubated on ice. As control, Triton-X-100 was additionally added. At the indicated time-points, aliquots were removed and subjected to Western blot analysis.

adding detergent, thereby corroborating its cytosolic localization in the absence of PEX14 (Figure 6F). A similar picture was obtained for FOX2, albeit the protein was degraded more slowly in the absence of Triton-X-100.

Finally, the localization of HEX1 and several glyoxysomal marker proteins was determined by immunofluorescence analysis. Antibodies against PEX14 gave rise to a punctate staining pattern in the wild-type strain (Figure 7), whereas only a weak diffuse staining was achieved in case of the *pex14Δ* mutant that did not differ much from background staining. HEX1 localized to a few large punctate structures in the wild type but was dispersed throughout the cytosol in the absence of PEX14, suggesting that Woronin body formation is entirely dependent on this peroxin. Visualization of the glyoxysomal matrix protein FOX2 in wild-type hyphae led to a punctate staining pattern that changed in *pex14*-deficient hyphae to a largely cytosolic staining in accord with a role for PEX14 in the targeting of glyoxysomal FOX2. Finally, a punctate staining was achieved for the membrane protein PEX13 in both the wild-type and the *pex14Δ* mutant strain (Figure 7), suggesting that PEX14 is not involved in the targeting of glyoxysomal membrane proteins.

PTS1-dependent targeting of HEX1 to Woronin bodies and glyoxysomes

Because PEX14 was required for the targeting of HEX1 although it was virtually absent from Woronin body membranes, topogenesis of HEX1 might require preceding import into glyoxysomes. To analyze this, a green fluorescent protein (GFP) fusion of HEX1 was expressed from the *ccg1* promoter in a wild-type strain. Detection of the fusion protein by Western blot revealed that it had the expected size of approximately 47 kDa, with an expression level below that of endogenous HEX1 (Figure S4). It has been shown recently that expressing *hex1* from the *ccg1* promoter that is most active in basal regions of a colony suffices to provoke Woronin body formation in these regions, although Woronin bodies typically emerge in apical regions of hyphae (30). GFP-HEX1 gave rise to large spots that colocalized with Woronin bodies as seen in

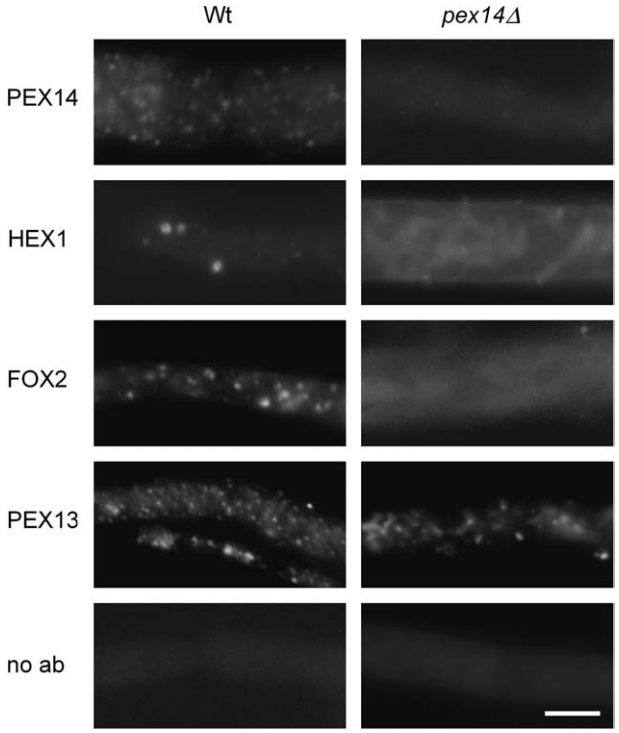

Figure 7: Role of PEX14 in the localization of HEX1 and glyoxysomal marker proteins. Wild-type and *pex14Δ* hyphae grown in minimal sucrose-containing medium were processed for indirect immunofluorescence microscopy with rabbit antibodies against PEX14, HEX1, FOX2 and PEX13. As a negative control, the primary antibody was omitted (no ab). The secondary antibody used was Alexa Fluor 594-labeled anti-rabbit IgG. Bar = 5 μm.

bright-field microscopy (Figure 8A). Fluorescent spots were also localized to septal pores (Figure 8B), likely capturing the event of septum clogging after hyphal wounding. The observed subcellular localization therefore indicated that the fusion protein was properly targeted. In a significant number of cells, smaller green spots were additionally observed that did not colocalize with discernible mature Woronin bodies (Figure 8A,C) and thus might represent Woronin body precursor structures.

Removing the C-terminal tripeptide SRL of HEX1, a canonical PTS1, gave rise to a diffuse fluorescence pattern and even Woronin bodies plugging the septal pore were not stained (Figure 8D). Because the smaller spots also vanished in the absence of HEX1's C-terminal three amino acids, targeting of HEX1 to Woronin bodies was entirely dependent on its canonical PTS1. This is likely to require recognition by the PTS1 receptor PEX5. Indeed, full-length HEX1 interacted with yeast PEX5 in a two-hybrid assay (Figure 8E). To find out whether the small GFP-HEX1-labeled spots represent glyoxysomes, double-immunofluorescence microscopy was used. A limited overlap was indeed observed for GFP-HEX1 and PEX14 (Figure 8F). Besides that, the PEX14 antibody occasionally stained foci from where the Woronin bodies seemed to emanate.

The subcellular localization of GFP-HEX1 was also analyzed via density gradient fractionation using PNS from oleic acid-induced hyphae. Localization of the fusion protein to Woronin bodies was confirmed as it clearly cosedimented with endogenous HEX1 (Figure 9). By contrast to the endogenous HEX1, a significant fraction of GFP-HEX1 cosedimented with the glyoxysomal marker proteins FOX2 and PEX14, in line with an import of GFP-HEX1 also into glyoxysomes. The observed dual location of GFP-HEX1 therefore suggested that topogenesis of HEX1 indeed occurs through this organelle.

Discussion

Microbodies are ubiquitous multipurpose organelles whose specialization can lead to the development of diverse organelles. Filamentous ascomycetes possess within a single cell two such compartments with a completely different matrix protein content, glyoxysomes and Woronin bodies. Here we show that the biogenesis of both types of organelles depends on the peroxin PEX14, a central component of the peroxisomal matrix protein import machinery.

The absence of functional glyoxysomes was inferred from the inability of *pex14Δ* mutants to grow on oleic acid as sole carbon source. A defect in peroxisome biogenesis usually results in a failure to degrade those fatty acids that are substrates for the peroxisomal β-oxidation system (47), which is only able to exert its function within peroxisomes. The non-growth phenotype of the *pex14Δ* mutant on oleic acid therefore supports the notion that *N. crassa* degrades fatty acids only within glyoxysomes (3). In apparent contrast, its close relative *Aspergillus nidulans* was suggested to possess an additional mitochondrial β-oxidation system that contributes to the degradation of oleic acid (48).

The *pex14Δ* mutant also suffered from losing cytoplasm on sucrose-containing VMM plates. This was probably because of the absence of Woronin bodies, which would normally seal septal pores in case of hyphal injury. Cytoplasmic bleeding has been described for the Woronin body-deficient *hex1*^{RIP} strain on sorbose plates (7,8), where hyphal branching, and as a consequence hyphal damage, is enhanced. Our notion that both the *hex1*^{RIP} as well as the *pex14Δ* mutant already showed some bleeding on sucrose-containing plates indicated that even infrequent branching imposes problems to a colony lacking Woronin bodies.

From the outset it appeared plausible that PEX14 is essential for the protein import into glyoxysomes but not into Woronin bodies or vice versa. However, both glyoxysomal malate synthase as well as the dominant protein of the Woronin body, HEX1, were completely mislocalized in the absence of PEX14. Thus, the same import machinery acts upon matrix proteins destined to either of the two organelles, thereby corroborating the relatedness of

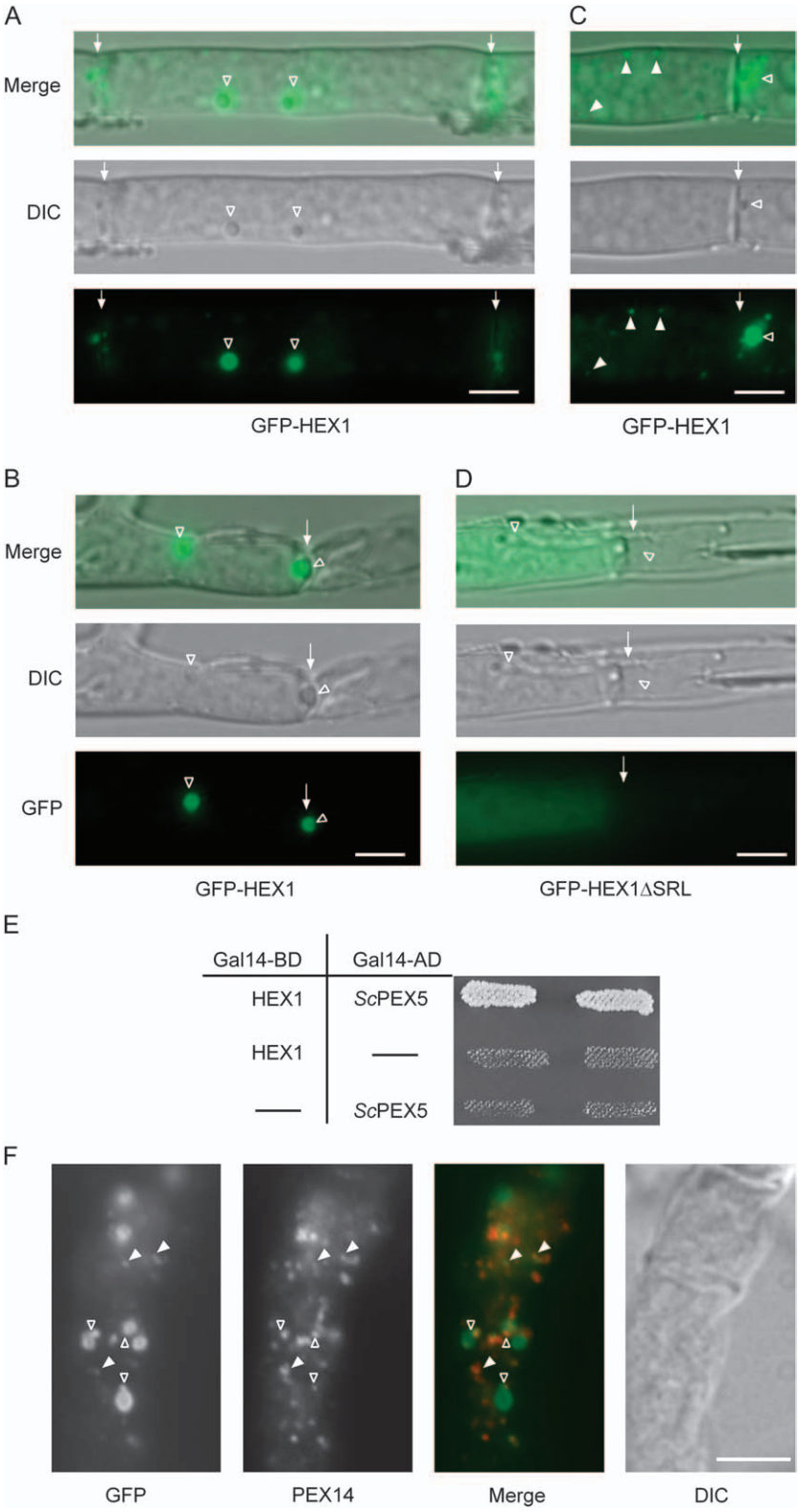

Figure 8: Subcellular localization of GFP-HEX1 and the role of its C-terminal tripeptide. A–D) *Neurospora crassa* wild-type mycelia expressing GFP-HEX1, grown in minimal sucrose-containing medium, were scrutinized for GFP-dependent fluorescence and the appearance of Woronin bodies through light microscopy. Arrows indicate septa with Woronin bodies in proximity. Open arrowheads mark Woronin bodies, whereas closed arrowheads denote smaller spots that do not colocalize with mature Woronin bodies and presumably represent glyoxysomes. A, B) Colocalization of GFP-HEX1 with Woronin bodies. C) Appearance of GFP-HEX1 in Woronin bodies and in smaller spots. D) Dependence of GFP-HEX1 targeting on its C-terminal SRL tripeptide (GFP-HEX1ΔSRL). In (B) and (D), a Woronin body has plugged the septal pore in response to an injury of the right segment. E) Interaction of HEX1 with the PTS1 receptor *Sc*PEX5 in a two-hybrid assay. The indicated plasmid combinations were analyzed as described for Figure 1. F) Double labeling of GFP-HEX1 and PEX14. The GFP-HEX1-expressing strain was subjected to double-immunofluorescence microscopy to localize GFP-HEX1 in tandem with glyoxysomal PEX14. Detection was achieved with mouse monoclonal antibodies against GFP combined with rabbit anti-PEX14 antibodies. The secondary antibodies used were Alexa Fluor 488-labeled anti-mouse IgG and Alexa Fluor 594-labeled anti-rabbit IgG. Closed arrowheads denote spots with an apparent colocalization of GFP-HEX1 and PEX14, whereas open arrowheads indicate PEX14-labeled foci that are associated with Woronin bodies. DIC, differential interference contrast; Bar = 5 μm.

Woronin bodies with microbodies (49). At the same time, these observations excluded PEX14 as a selectivity factor that would establish the two distinct compartments within a cell. Inactivation of the peroxisomal protein import machinery in *Arabidopsis thaliana* through deletion of *pex14* likewise revealed that the same import machinery is used for glyoxysomes, leaf peroxisomes and unspecialized peroxisomes (50). In this case, however, the

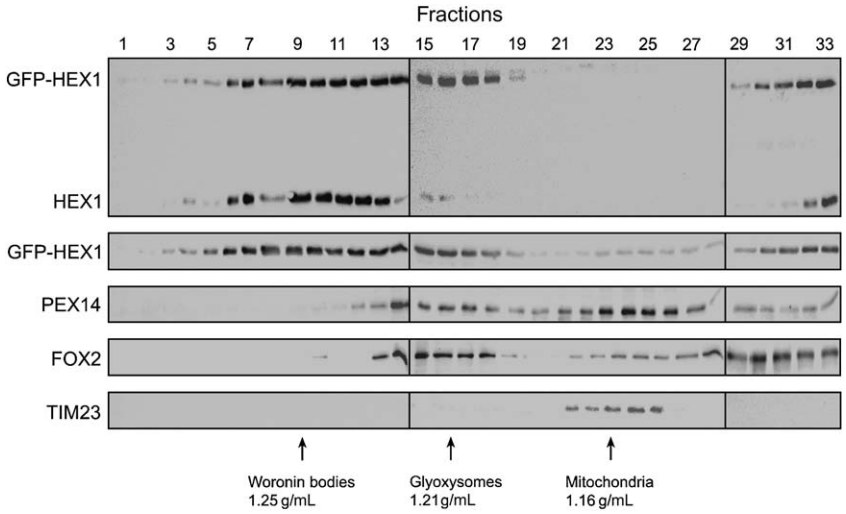

Figure 9: Subcellular distribution of GFP-HEX1 in oleic acid-induced cells. Extract of oleic acid-induced *Neurospora crassa* mycelia expressing GFP-HEX1 was subjected to 30–60% (w/w) sucrose density gradient centrifugation at 38 000 × ***g*** for 2 h. One-milliliter fractions were collected from the bottom (fraction 1) to the top and analyzed for the distribution of GFP-HEX1, endogenous HEX1, glyoxysomal PEX14 and FOX2, as well as mitochondrial TIM23 by Western blot. GFP-HEX1 was detected with antibodies against HEX1 (top panel) and GFP (bottom panel). The peak fractions of Woronin bodies, glyoxysomes and mitochondria are indicated. GFP-HEX1 was dually localized to Woronin bodies and glyoxysomes.

different kinds of microbodies are converted into one another through the co-ordinated expression (and degradation) of distinct sets of proteins in dependence of the developmental state and tissue type and are not encountered in a cell at the same time.

The essential role of PEX14 in the topogenesis of HEX1 is remarkable insofar as neither PEX14 nor PEX13 was localized to Woronin bodies in appreciable amounts. As a consequence, Woronin bodies are probably not import-competent and constitute dead-end organelles. This may ensure that once formed, Woronin bodies are unable to import glyoxysomal matrix proteins. Such an exclusion of unscheduled proteins from Woronin bodies would also serve to maintain this specialized organelle concomitantly with glyoxysomes.

To understand how Woronin bodies are differentiated from glyoxysomes, the role glyoxysomes play in the topogenesis of HEX1 must be considered. Jedd and Chua (8) reported that a GFP fusion of HEX1 targets to peroxisomes of *S. cerevisiae* (an organism lacking Woronin bodies) in a PTS1-dependent manner. We show in this work that the C-terminal tripeptide SRL of HEX1 also works in the native context as it proved essential to direct GFP-HEX1 to mature Woronin bodies. The fluorescence-labeled organelles were found at the cell periphery or, in case of a hyphal burst, at the septal pore, which was in agreement with the observations made with a DsRed2-HEX1 fusion protein in *Aspergillus oryzae* (51). We found evidence that the fusion protein also localized to glyoxysomes: in addition to the large punctate structures that were congruent with Woronin bodies, small spots were discernible, some of which colocalized with PEX14. In the absence of HEX1's C-terminal tripeptide also these small spots vanished. Furthermore, in a density gradient, a portion of GFP-HEX1 was detected in the fractions of glyoxysomal marker proteins. Although it remains possible that GFP-HEX1 was mistargeted to glyoxysomes because of its ectopic expression, it is more likely that the observation made reflected a transient glyoxysomal residence of HEX1 en route to Woronin bodies.

Pioneer electron microscopic analysis of the filamentous fungus *Fusarium oxysporum* recorded the formation of bulges from microbodies that were filled with an electron-dense matrix. The eventual separation of this inclusion (i.e. the formation of Woronin bodies) was suggested to occur by an exocytotic mechanism (29). More recently, transient association of the synthetic glyoxysomal marker protein GFP-SKL with core Woronin bodies was seen under the light microscope (30). These hybrid organelles were subject to an apparent fission of the Woronin body from the GFP-SKL-marked vesicles. We noted that endogenous HEX1 was virtually absent from glyoxysomal fractions, indicating that such hybrid organelles are short-lived entities. By contrast, the GFP-HEX1 fusion was readily detectable in these fractions. We theorize that the GFP moiety adversely affected the crystallization or condensation of GFP-HEX1 within glyoxysomes, thereby fortuitously slowing down the formation of Woronin bodies. The occasional appearance of PEX14-labeled foci close to GFP-HEX1-containing Woronin bodies supports this idea. Taken together, all experimental evidence can be reconciled with the formation of Woronin bodies through a preceding import of HEX1 into glyoxysomes. Because in this case HEX1 and possibly other Woronin body-specific proteins need to be separated from resident proteins within glyoxysomes, a search for factors that selectively promote this process could be a promising approach.

Of interest, the *pex14Δ* mutant appeared to exhibit a differential import defect in that the PTS1 proteins HEX1 and MLS1 were exclusively detected in the cytosol, whereas FOX2 and ICL1, both of which lack a typical PTS, were also detected in organellar fractions. The largely diffuse labeling seen for FOX2 in *pex14* cells, however, argues against a significant glyoxysomal import at least of

this matrix protein. Whether import of PTS2 proteins depends on PEX14 remains to be determined; the observed interaction of PEX14 with the PTS2 receptor PEX7 in the two-hybrid assay suggests that this is indeed the case.

A last point that warrants discussion is the observed presence of glyoxysomal vesicles of heterogeneous density and protein composition. Whereas all tested marker proteins sedimented with the mature, high-density glyoxysomes, particularly PEX14 was also present in lighter fractions. In *Yarrowia lipolytica*, two light peroxisomal precursor vesicles with distinct sets of matrix proteins were isolated that eventually fuse in the process of peroxisome maturation (52,53). We speculate that such pools of glyoxysomal precursor vesicles also exist in *N. crassa*. In light of the rather prominent appearance of such vesicles, *N. crassa* could be also well suited to test whether peroxisomes indeed emanate through budding from the endoplasmic reticulum, a hypothesis that gained weight by a number of recent studies (54–57).

In summary, we have shown here that the typical peroxisomal import machinery is used for the import of HEX1 and that the absence of a single component of this machinery prevents the formation of functional glyoxysomes and Woronin bodies. The virtual absence of peroxins in Woronin bodies together with the observation that HEX1 was also imported into glyoxysomes supports at the molecular level the view that Woronin bodies emerge from glyoxysomes by fission.

Materials and Methods

Strains and culture conditions

Neurospora crassa strains FGSC 987 (St Lawrence 74-OR23-1A, *mat A*), FGSC 988 (St Lawrence 74-OR8-1a, *mat a*), FGSC 6103 (N623, *his-3 mat A*), FGSC 8612 (*hex1*^{RIP} *mat a*) and the *pex14Δ* gene deletion strains FGSC 11304 (*pex14::hph mat A*) and FGSC 11305 (*pex14::hph mat a*) were obtained from the Fungal Genetics Stock Center (Kansas City, KS, USA). The last two strains were generated in the course of the Neurospora Gene Knockout Project (58). Correct replacement of *pex14* by the hygromycin resistance gene (*hph*) cassette was verified by polymerase chain reaction (PCR) using primer pair RE571/572.

Strains expressing eGFP-HEX1 (Nc18) or eGFP-HEX1ΔSRL (Nc22) were generated by integration of the linearized plasmids pCW15 and pCW18, respectively, into the *his-3* locus of strain N623 by homologous recombination, followed by a screening of prototrophic His$^+$ transformants for expression of the respective eGFP fusion protein by immunoblotting. The strain ectopically expressing His$_6$-PEX14 (Nc3) was generated by transformation of wild-type strain 74-OR23-1A with linearized plasmid pMAR24, followed by a screening of BASTA-resistant colonies for the overexpression of His$_6$-PEX14.

All manipulations including crossing were carried out according to standard techniques for *N. crassa* (59). For growth in liquid medium, strains were inoculated with 10^5 conidia/mL (or in the case of the *pex14Δ* mutant with small mycelia-containing pieces of agar) in VMM supplemented with 2% sucrose (w/v) and shaken (100 rpm) at 30°C for 24 h. For the induction of glyoxysomes, hyphae were harvested by filtration, shifted to VMM supplemented with 2% (v/v) ethanol or 3 mM oleic acid plus 0.1% (w/v) Tween-40 and shaken for another 12 h.

For growth tests, small pieces of mycelia 0.5 cm in diameter were inoculated at the edge of large Petri dishes. VMM was supplemented with 2% sucrose, 2% ethanol or 0.1% oleic acid plus 0.05% Tergitol NP-40 (Sigma-Aldrich, St Louis, MO, USA) as carbon sources. The plates were incubated at 30°C for up to 4 days with alternating light (10 h) and dark (14 h) periods. To determine the average growth rate, the growth fronts were marked every 2 h within the 10-h light periods.

The *S. cerevisiae* wild-type strain UTL-7A and the otherwise isogenic *pex14Δ* mutant (36), as well as the two-hybrid strain PJ69-4a, obtained from P. James, Madison, and used, for instance, in Rottensteiner et al. (60), have been described. *Escherichia coli* strain DH5α was used for all plasmid amplifications and isolations. Standard media for the cultivation of yeast and bacterial strains were prepared as described (61).

Plasmids and cloning procedures

All plasmids and oligonucleotides used are listed in Table S1. The cDNAs of *pex7*, *pex13*, *pex14* and *hex1* were amplified from an *N. crassa* cDNA library by PCR. The open reading frames of *pex13* (NCU02618.3) and *pex14* (NCU03901.3) were adopted from the prediction by Assembly 7 of the *Neurospora* genome sequence (http://www.broad.mit.edu/annotation/fungi/neurospora_crassa_7/index.html). The respective genomic DNA segments were similarly amplified, but with DNA isolated from wild-type strain 74-OR23-1A as a template. Genes or gene fragments were cloned into the various expression vectors using the restriction sites and primer pairs as indicated in Table S1. The identities of all PCR-generated fragments were verified by automated sequencing (MWG-BIOTECH AG, Ebersberg, Germany).

Generation and usage of antisera

Antibodies against GFP (60), *S. cerevisiae* Mls1p (62), *A. gossypii* Icl1p (63), *N. crassa* FOX2 (64), TIM23 (65), HEX1 (8) and AAC2 (66) have been described. Antibodies against PEX13 and PEX14 were generated through immunization of rabbits with appropriate recombinant proteins. In the case of PEX13, its SH3 domain was expressed as a glutathione S-transferase (GST) fusion protein from plasmid pMAR25 in *E. coli*. Purification with GST Sepharose was carried out according to manufacturer's instructions (GE Healthcare, Freiburg, Germany). PEX14 was similarly expressed as a GST fusion protein from pMAR16. Because GST-PEX14 failed to bind to GST Sepharose, it was purified over a Ni-NTA column (Qiagen, Hilden, Germany) under denaturing conditions by virtue of a hexahistidine tag that had been introduced right after the GST moiety (GST-H$_6$-PEX14). Immunoreactive complexes were visualized using anti-rabbit IgG-coupled horseradish peroxidase in combination with the ECL™ system from GE Healthcare.

Preparation of an N. crassa PNS, protease protection assay, differential and density gradient centrifugation and Woronin body purification

Neurospora crassa hyphae were harvested by filtration, washed with water, mixed with 1 g/g wet weight quartz sand and 4 volumes of isolation buffer [150 mM Tricine, pH 7.4, 0.44 M sucrose, 10 mM KCl, 5 mM $MgCl_2$, 1 mM ethylenediaminetetraacetic acid (EDTA)] plus protease inhibitors (8 μM antipain, 0.3 μM aprotinin, 1 mM benzamidine, 1 μM bestatin, 10 μM chymostatin, 5 μM leupeptin, 1.5 μM pepstatin and 1 mM phenylmethylsulfonyl fluoride) and ground with a pestle in a mortar at 4°C. The homogenate was squeezed through four layers of cheesecloth and centrifuged three times at 500 × ***g*** for 5 min. The resulting supernatant was taken as PNS.

Protease protection assays were carried out by treating ice-cold PNS with 100 μg/mL proteinase K in the presence or absence of Triton-X-100. Aliquots were removed after 0, 5, 10, 15 and 30 min and treated with PMSF to stop the reaction. Samples were subjected to trichloroacetic acid precipitation and analyzed by Western blot.

For differential centrifugation, the PNS was subjected to consecutive centrifugation steps with increasing speed and time (1000 × ***g***, 5 min; 5000 × ***g***, 10 min; 10 000 × ***g***, 15 min; 25 000 × ***g*** 30 min; 100 000 × ***g***, 1 h). Proportional volumes of the PNS, the resulting pellets and the final supernatant were analyzed by Western blot. Alternatively, the PNS was separated by centrifugation at 27 000 × ***g*** for 20 min and thereafter at 200 000 × ***g*** for 1 h. Here, samples with equal protein content were subjected to Western blot analysis.

For the separation of organelles by density gradient centrifugation, 10 mL of PNS was layered on top of a linear gradient of 30–60% (w/w) sucrose, dissolved in buffer containing 10 mM Tricine, pH 7.4, 1 mM EDTA. Alternatively, a 10–35% (w/v) Nycodenz® (Axis-Shield, Oslo, Norway) gradient, dissolved in the same buffer but additionally supplied with 0.25 mM sucrose, was used. The gradients were subjected to centrifugation for 2 h at 40 000 × ***g*** at 4°C in a Sorvall SV288 vertical rotor. Fractions of 1 mL were collected from the bottom to the top and densities were determined refractometrically. Aliquots of each fraction were processed for SDS–PAGE and analyzed by Western blot.

To purify Woronin bodies, a 10 000 × ***g*** pellet was prepared from a PNS of sucrose-grown wild-type cells. Following resuspension, the pellet was loaded on top of a 52% (w/w) sucrose cushion (1.25 g/mL) and subjected to centrifugation at 48 000 × ***g*** at 4°C for 1 h. The resulting pellet enriched for Woronin bodies was again resuspended and subjected to sucrose density gradient centrifugation as described previously.

Isolation of His_6-PEX14

To isolate His_6-PEX14, PNS from sucrose-grown mycelia of strain Nc3 and a wild-type control strain were prepared as described previously but using lysis buffer (20 mM Tris–HCl, pH 8.0, 300 mM NaCl, 10% (w/v) glycerol, protease inhibitors as described previously) supplied with 10 mM imidazole. The PNS was subjected to centrifugation at 100 000 × ***g*** for 1 h, and the membrane pellet fraction was solubilized with 1% digitonin (w/v) at 4°C for 1 h. Following centrifugation (100 000 × ***g***, 1 h), the supernatant fraction was subjected to affinity chromatography using Ni-NTA matrix (Qiagen). Bound His_6-PEX14 was washed twice with lysis buffer containing 20 and 40 mM imidazole and eluted with 150 mM imidazole dissolved in lysis buffer without protease inhibitors. Aliquots of each step were processed for SDS–PAGE and analyzed by Western blot for the presence of His_6-PEX14 and other proteins eventually coisolated.

Fluorescence microscopy

For the inspection of *N. crassa* mycelia, strains were grown overnight in VMM. For live cell imaging, a suspension of mycelia was placed on a slide, mixed with an equal volume of 1% (w/v) low-melting agarose in H_2O and sealed with a coverslip. For indirect immunofluorescence, mycelium from liquid cultures grown for 24–48 h was fixed in 3.7% paraformaldehyde for 30–40 min (67). After several washes with buffer 1 (1× PBS, 0.2 M glycine), the mycelium was treated basically as described in Seiler et al. (68) with 10 mg/mL cell wall digesting enzymes (Lysing enzymes, Sigma) and 10 mg/mL BSA dissolved in buffer 2 (100 mM potassium citrate, pH 6.0, 200 mM KCl, 20 mM EGTA) for 10–30 min. The mycelium was rinsed several times in buffer 2 before the partially permeabilized hyphae were incubated with blocking solution (10% BSA in buffer 2) for at least 1 h at room temperature to block non-specific binding of antibodies. Thereafter, hyphae were incubated with primary antibodies dissolved in blocking solution for 8 h at room temperature. Hyphae were washed several times with buffer 2 before they were incubated with the secondary antibodies for 8 h in blocking buffer. After three washing steps with buffer 2, cells were inspected under the microscope. Secondary antibodies were obtained from Molecular Probes (Eugene, OR, USA; Alexa Fluor 594 goat anti-rabbit IgG and Alexa Fluor 488 goat anti-mouse IgG). The primary antibodies used were α-HEX1 (1:500), α-FOX2 (1:1000), α-PEX14 (1:500), α-PEX13 (1:500) and α-GFP (1:100). All micrographs were recorded on a Zeiss Axioplan 2 microscope with a Zeiss Plan-Apochromat ×100/1.4 oil objective and an Axiocam MR digital camera and were processed with AxioVision 4.2 software (Zeiss, Jena, Germany).

Electron microscopy

For overall cell morphology, hyphae grown in oleic acid (wild type) or ethanol (*hex1^{RIP}* and *pex14Δ*) were fixed in 1.5% $KMnO_4$ for 20 min, poststained in 0.5% uranylacetate, subsequently dehydrated via an ethanol series and embedded in Epon 812. For immunocytochemistry, oleic acid-induced hyphae were fixed with glutaraldehyde and embedded in Unicryl. Ultrathin sections were then incubated with specific anti-HEX1 or anti-FOX2 antibodies and gold-conjugated goat-anti rabbit antiserum as described (69).

Miscellaneous

The following procedures were carried out as described: yeast two-hybrid analysis (60), preparation of yeast whole-cell extracts (70), transformation of yeast cells (71) and the transformation of *N. crassa* spheroplasts by electroporation (59).

Acknowledgments

We thank A. Hartig, G. Jedd, K.-P. Stahmann and D. Mokranjac for antibodies; F. Nargang for the cDNA library; H. Germeroth and H. Prokisch for the generation of *N. crassa* strain Nc3; M. Freitag for plasmid pMF272 (72), and H. Colot for prioritizing the preparation of the *pex14Δ* knockout strain. We further thank M. Nowrousian for critical reading of the manuscript. Special gratitude is expressed for R. Erdmann's general support. This work was supported by grants from the Deutsche Forschungsgemeinschaft (project B10 of SFB480).

Supplementary Materials

Figure S1: Alignment of PEX13 with yeast orthologs. PEX13 sequences from *Neurospora crassa* (NCU02618.3; *Nc*PEX13), *Pichia pastoris* (Q92266; *Pp*PEX13) and *Saccharomyces cerevisiae* (YLR191w; *Sc*PEX13) were used to perform a multiple sequence alignment using ClustalW with its default parameters (http://www.ebi.ac.uk/clustalw/). Identical amino acids are shaded in black and similar ones in gray using BoxShade (http://www.ch.embnet.org/software/BOX_form.html).

Figure S2: Alignment of PEX14 with yeast orthologs. PEX14 sequences from *Neurospora crassa* (NCU03901.3; *Nc*PEX14), *Pichia pastoris* (AAG28574; *Pp*PEX14) and *Saccharomyces cerevisiae* (YGL153w; *Sc*PEX14) were used to perform a multiple sequence alignment using ClustalW with its default parameters. Identical amino acids are shaded in black and similar ones in gray using BoxShade.

Figure S3: Specificity of antibodies generated against PEX14 and PEX13. (A, B) PEX14 antibody test. Antisera generated against a recombinant GST fusion of *N. crassa* PEX14 were tested for specificity using whole-cell extracts prepared from the oleic acid-induced *S. cerevisiae* wild-type strain UTL-7A, an otherwise isogenic *pex14* mutant strain, and the *pex14* mutant expressing *Nc*PEX14 (A). An identical blot was also decorated with anti-*Sc*PEX14 antibodies (B). *Nc*PEX14 was detected by both antibodies (black arrows) whereas yeast PEX14 was only recognized by anti-*Sc*PEX14 antibodies (open arrows). The second band of approximately 29 kDa represents a stable degradation product of *Sc*PEX14. Analysis of post-nuclear supernatants from *N. crassa* wild type and a *pex14* mutant also revealed a PEX14-specific band of 47 kDa (A). (C) PEX13 antibody test. Antisera against a recombinant GST fusion of the SH3 domain of PEX13 were similarly tested for specificity using whole-cell extracts from two-hybrid strain PJ69-4a that had expressed Gal4 DNA-binding or activation domain fusions of the SH3 domain of PEX13 (AD-SH3, BD-SH3), full-length PEX13 (BD-PEX13), or PEX14 (AD-PEX14). *N.c.* = *N. crassa* extract; *S.c.* = *S. cerevisiae* extract.

Figure S4: **Expression of GFP-HEX1.** Correct expression of the fusion protein was determined by Western blotting using anti-HEX1 (left panel) and anti-GFP (right panel) antibodies. The amount of endogenous HEX1 exceeded that of GFP-HEX1.

Table S1: **Plasmids and oligonucleotides used.**

Supplemental materials are available as part of the online article at http://www.blackwell-synergy.com

References

1. van den Bosch H, Schutgens RB, Wanders RJ, Tager JM. Biochemistry of peroxisomes. Annu Rev Biochem 1992;61:157–197.
2. Titorenko VI, Rachubinski RA. The peroxisome: orchestrating important developmental decisions from inside the cell. J Cell Biol 2004;164: 641–645.
3. Kionka C, Kunau W-H. Inducible β-oxidation pathway in *Neurospora crassa*. J Bacteriol 1985;161:153–157.
4. Parsons M. Glycosomes: parasites and the divergence of peroxisomal purpose. Mol Microbiol 2004;53:717–724.
5. Borst P. How proteins get into microbodies (peroxisomes, glyoxysomes, glycosomes). Biochim Biophys Acta 1986;866:179–203.
6. Yuan P, Jedd G, Kumaran D, Swaminathan S, Shio H, Hewitt D, Chua NH, Swaminathan K. A HEX-1 crystal lattice required for Woronin body function in *Neurospora crassa*. Nat Struct Biol 2003;10:264–270.
7. Tenney K, Hunt I, Sweigard J, Pounder JI, McClain C, Bowman EJ, Bowman BJ. Hex-1, a gene unique to filamentous fungi, encodes the major protein of the Woronin body and functions as a plug for septal pores. Fungal Genet Biol 2000;31:205–217.
8. Jedd G, Chua NH. A new self-assembled peroxisomal vesicle required for efficient resealing of the plasma membrane. Nat Cell Biol 2000;2: 226–231.
9. Markham P, Collinge AJ. Woronin bodies of filamentous fungi. FEMS Microbiol Rev 1987;46:1–11.
10. Hayashi M, Toriyama K, Kondo M, Kato A, Mano S, De Bellis L, Hayashi-Ishimaru Y, Yamaguchi K, Hayashi H, Nishimura M. Functional transformation of plant peroxisomes. Cell Biochem Biophys 2000;32: 295–304.
11. Wanner G, Theimer RR. Two types of microbodies in *Neurospora crassa*. Ann N Y Acad Sci 1982;386:269–284.
12. Soundararajan S, Jedd G, Li X, Ramos-Pamplona M, Chua NH, Naqvi NI. Woronin body function in *Magnaporthe grisea* is essential for efficient pathogenesis and for survival during nitrogen starvation stress. Plant Cell 2004;16:1564–1574.
13. Gould SJ, Keller GA, Hosken N, Wilkinson J, Subramani S. A conserved tripeptide sorts proteins to peroxisomes. J Cell Biol 1989;108: 1657–1664.
14. Lametschwandtner G, Brocard C, Fransen M, Van Veldhoven P, Berger J, Hartig A. The difference in recognition of terminal tripeptides as peroxisomal targeting signal 1 between yeast and human is due to different affinities of their receptor Pex5p to the cognate signal and to residues adjacent to it. J Biol Chem 1998;273:33635–33643.
15. Swinkels BW, Gould SJ, Bodnar AG, Rachubinski RA, Subramani S. A novel, cleavable peroxisomal targeting signal at the amino-terminus of the rat 3-ketoacyl-CoA thiolase. EMBO J 1991;10:3255–3262.
16. Klein AT, van den Berg M, Bottger G, Tabak HF, Distel B. *Saccharomyces cerevisiae* acyl-CoA oxidase follows a novel, non-PTS1, import pathway into peroxisomes that is dependent on Pex5p. J Biol Chem 2002;277: 25011–25019.
17. Schäfer A, Kerssen D, Veenhuis M, Kunau WH, Schliebs W. Functional similarity between the peroxisomal PTS2 receptor binding protein Pex18p and the N-terminal half of the PTS1 receptor Pex5p. Mol Cell Biol 2004;24:8895–8906.
18. Heiland I, Erdmann R. Biogenesis of peroxisomes. Topogenesis of the peroxisomal membrane and matrix proteins. FEBS J 2005;272: 2362–2372.
19. Erdmann R, Schliebs W. Peroxisomal matrix protein import: the transient pore model. Nat Rev Mol Cell Biol 2005;6:738–742.
20. Sacksteder KA, Gould SJ. The genetics of peroxisome biogenesis. Annu Rev Genet 2000;34:623–652.
21. Purdue PE, Lazarow PB. Peroxisome biogenesis. Annu Rev Cell Dev Biol 2001;17:701–752.
22. Baker A, Sparkes IA. Peroxisome protein import: some answers, more questions. Curr Opin Plant Biol 2005;8:640–647.
23. Sichting M, Schell-Steven A, Prokisch H, Erdmann R, Rottensteiner H. Pex7p and Pex20p of *Neurospora crassa* function together in PTS2-dependent protein import into peroxisomes. Mol Biol Cell 2003;14: 810–821.
24. Leon S, Zhang L, McDonald WH, Yates J III, Cregg JM, Subramani S. Dynamics of the peroxisomal import cycle of PpPex20p: ubiquitin-dependent localization and regulation. J Cell Biol 2006;172:67–78.
25. Einwächter H, Sowinski S, Kunau WH, Schliebs W. *Yarrowia lipolytica* Pex20p, *Saccharomyces cerevisiae* Pex18p/Pex21p and mammalian Pex5pL fulfil a common function in the early steps of the peroxisomal PTS2 import pathway. EMBO Rep 2001;2:1035–1039.
26. Titorenko VI, Smith JJ, Szilard RK, Rachubinski RA. Pex20p of the yeast *Yarrowia lipolytica* is required for the oligomerization of thiolase in the cytosol and for its targeting to the peroxisome. J Cell Biol 1998;142: 403–420.
27. Gunkel K, van Dijk R, Veenhuis M., van der Klei IJ. Routing of *Hansenula polymorpha* alcohol oxidase: an alternative peroxisomal protein-sorting machinery. Mol Biol Cell 2004;15:1347–1355.
28. Kiel JA, Veenhuis M., van der Klei IJ. PEX genes in fungal genomes: common, rare or redundant. Traffic 2006;7:1291–1303.
29. Wergin WP. Development of Woronin bodies from microbodies in *Fusarium oxysporum f. sp. lycopersici*. Protoplasma 1973;76: 249–260.
30. Tey WK, North AJ, Reyes JL, Lu YF, Jedd G. Polarized gene expression determines Woronin body formation at the leading edge of the fungal colony. Mol Biol Cell 2005;16:2651–2659.
31. Galagan JE, Calvo SE, Borkovich KA, Selker EU, Read ND, Jaffe D, FitzHugh W, Ma LJ, Smirnov S, Purcell S, Rehman B, Elkins T, Engels R, Wang S, Nielsen CB et al. The genome sequence of the filamentous fungus *Neurospora crassa*. Nature 2003;422:859–868.
32. Chenna R, Sugawara H, Koike T, Lopez R, Gibson TJ, Higgins DG, Thompson JD. Multiple sequence alignment with the Clustal series of programs. Nucleic Acids Res 2003;31:3497–3500.
33. Girzalsky W, Rehling P, Stein K, Kipper J, Blank L, Kunau WH, Erdmann R. Involvement of Pex13p in Pex14p localization and peroxisomal targeting signal 2-dependent protein import into peroxisomes. J Cell Biol 1999;144:1151–1162.
34. Stein K, Schell-Steven A, Erdmann R, Rottensteiner H. Interactions of Pex7p and Pex18p/Pex21p with the peroxisomal docking machinery: implications for the first steps in PTS2 protein import. Mol Cell Biol 2002;22:6056–6069.
35. Otera H, Setoguchi K, Hamasaki M, Kumashiro T, Shimizu N, Fujiki Y. Peroxisomal targeting signal receptor Pex5p interacts with cargoes and import machinery components in a spatiotemporally differentiated manner: conserved Pex5p WXXXF/Y motifs are critical for matrix protein import. Mol Cell Biol 2002;22:1639–1655.
36. Albertini M, Rehling P, Erdmann R, Girzalsky W, Kiel JA, Veenhuis M, Kunau WH. Pex14p, a peroxisomal membrane protein binding both receptors of the two PTS-dependent import pathways. Cell 1997;89: 83–92.

37. Brocard C, Lametschwandtner G, Koudelka R, Hartig A. Pex14p is a member of the protein linkage map of Pex5p. EMBO J 1997;16: 5491–5500.
38. Fransen M, Terlecky SR, Subramani S. Identification of a human PTS1 receptor docking protein directly required for peroxisomal protein import. Proc Natl Acad Sci U S A 1998;95:8087–8092.
39. Reguenga C, Oliveira ME, Gouveia AM, Sa-Miranda C, Azevedo JE. Characterization of the mammalian peroxisomal import machinery: Pex2p, Pex5p, Pex12p, and Pex14p are subunits of the same protein assembly. J Biol Chem 2001;276:29935–29942.
40. Itoh R, Fujiki Y. Functional domains and dynamic assembly of the peroxin Pex14p, the entry site of matrix proteins. J Biol Chem 2006;281: 10196–10205.
41. Johnson MA, Snyder WB, Cereghino JL, Veenhuis M, Subramani S, Cregg JM. *Pichia pastoris* Pex14p, a phosphorylated peroxisomal membrane protein, is part of a PTS-receptor docking complex and interacts with many peroxins. Yeast 2001;18:621–641.
42. Schell-Steven A, Stein K, Amoros M, Landgraf C, Volkmer-Engert R, Rottensteiner H, Erdmann R. Identification of a novel, intraperoxisomal Pex14-binding site in Pex13: association of pex13 with the docking complex is essential for peroxisomal matrix protein import. Mol Cell Biol 2005;25:3007–3018.
43. Dunlap JC, Loros JJ. The *Neurospora* circadian system. J Biol Rhythms 2004;19:414–424.
44. Merrow M, Roenneberg T, Macino G, Franchi L. A fungus among us: the *Neurospora crassa* circadian system. Semin Cell Dev Biol 2001;12: 279–285.
45. Berteaux-Lecellier V, Picard M, Thompson-Coffe C, Zickler D, Panvier-Adoutte A, Simonet JM. A nonmammalian homolog of the *PAF1* gene (Zellweger syndrome) discovered as a gene involved in caryogamy in the fungus *Podospora anserina*. Cell 1995;81:1043–1051.
46. Trinci AP, Collinge AJ. Structure and plugging of septa of wild type and spreading colonial mutants of *Neurospora crassa*. Arch Mikrobiol 1973;91:355–364.
47. Erdmann R, Veenhuis M, Mertens D, Kunau WH. Isolation of peroxisome-deficient mutants of *Saccharomyces cerevisiae*. Proc Natl Acad Sci U S A 1989;86:5419–5423.
48. Maggio-Hall LA, Keller NP. Mitochondrial β-oxidation in *Aspergillus nidulans*. Mol Microbiol 2004;54:1173–1185.
49. Keller GA, Krisans S, Gould SJ, Sommer JM, Wang CC, Schliebs W, Kunau W, Brody S, Subramani S. Evolutionary conservation of a microbody targeting signal that targets proteins to peroxisomes, glyoxysomes, and glycosomes. J Cell Biol 1991;114:893–904.
50. Hayashi M, Nito K, Toriyama-Kato K, Kondo M, Yamaya T, Nishimura M. *At*Pex14p maintains peroxisomal functions by determining protein targeting to three kinds of plant peroxisomes. EMBO J 2000;19: 5701–5710.
51. Maruyama J, Juvvadi PR, Ishi K, Kitamoto K. Three-dimensional image analysis of plugging at the septal pore by Woronin body during hypotonic shock inducing hyphal tip bursting in the filamentous fungus *Aspergillus oryzae*. Biochem Biophys Res Commun 2005;331: 1081–1088.
52. Titorenko VI, Chan H, Rachubinski RA. Fusion of small peroxisomal vesicles in vitro reconstructs an early step in the in vivo multistep peroxisome assembly pathway of *Yarrowia lipolytica*. J Cell Biol 2000;148:29–44.
53. Titorenko VI, Mullen RT. Peroxisome biogenesis: the peroxisomal endomembrane system and the role of the ER. J Cell Biol 2006;174: 11–17.
54. Kunau WH. Peroxisome biogenesis: end of the debate. Curr Biol 2005;15:R774–R776.
55. Kim PK, Mullen RT, Schumann U, Lippincott-Schwartz J. The origin and maintenance of mammalian peroxisomes involves a de novo PEX16-dependent pathway from the ER. J Cell Biol 2006;173: 521–532.
56. Hoepfner D, Schildknegt D, Braakman I, Philippsen P, Tabak HF. Contribution of the endoplasmic reticulum to peroxisome formation. Cell 2005;122:85–95.
57. Haan GJ, Baerends RJ, Krikken AM, Otzen M, Veenhuis M, van der Klei IJ. Reassembly of peroxisomes in *Hansenula polymorpha pex3* cells on reintroduction of Pex3p involves the nuclear envelope. FEMS Yeast Res 2006;6:186–194.
58. Colot HV, Park G, Turner GE, Ringelberg C, Crew CM, Litvinkova L, Weiss RL, Borkovich KA, Dunlap JC. A high-throughput gene knockout procedure for *Neurospora* reveals functions for multiple transcription factors. Proc Natl Acad Sci U S A 2006;103:10352–10357.
59. Davies RH. Genetic, biochemical, and molecular techniques. In: Neurospora: Contributions of a Model Organism. Oxford University Press, New York; 2000, pp. 283–302.
60. Rottensteiner H, Kramer A, Lorenzen S, Stein K, Landgraf C, Volkmer-Engert R, Erdmann R. Peroxisomal membrane proteins contain common Pex19p-binding sites that are an integral part of their targeting signals. Mol Biol Cell 2004;15:3406–3417.
61. Sambrook J, Fritsch EF, Maniatis T. Molecular Cloning: A Laboratory Manual. Cold Spring Harbor, NY: Cold Spring Harbor Laboratory Press; 1989.
62. Hartig A, Simon MM, Schuster T, Daugherty JR, Yoo HS, Cooper TG. Differentially regulated malate synthase genes participate in carbon and nitrogen metabolism of *S. cerevisiae*. Nucleic Acids Res 1992;20:5677–5686.
63. Maeting I, Schmidt G, Sahm H, Revuelta JL, Stierhof YD, Stahmann KP. Isocitrate lyase of *Ashbya gossypii* – transcriptional regulation and peroxisomal localization. FEBS Lett 1999;444:15–21.
64. Thieringer R, Kunau WH. The β-oxidation system in catalase-free microbodies of the filamentous fungus *Neurospora crassa*. Purification of a multifunctional protein possessing 2-enoyl-CoA hydratase, L-3-hydroxyacyl-CoA dehydrogenase, and 3-hydroxyacyl-CoA epimerase activities. J Biol Chem 1991;266:13110–13117.
65. Mokranjac D, Paschen SA, Kozany C, Prokisch H, Hoppins SC, Nargang FE, Neupert W, Hell K. Tim50, a novel component of the TIM23 preprotein translocase of mitochondria. EMBO J 2003;22:816–825.
66. Palmieri L, Rottensteiner H, Girzalsky W, Scarcia P, Palmieri F, Erdmann R. Identification and functional reconstitution of the yeast peroxisomal adenine nucleotide transporter. EMBO J 2001;20: 5049–5059.
67. Rosa AL, Alvarez ME, Lawson D, Maccioni HJ. A polypeptide of 59 kDa is associated with bundles of cytoplasmic filaments in *Neurospora crassa*. Biochem J 1990;268:649–655.
68. Seiler S, Vogt N, Ziv C, Gorovits R, Yarden O. The STE20/germinal center kinase POD6 interacts with the NDR kinase COT1 and is involved in polar tip extension in *Neurospora crassa*. Mol Biol Cell 2006;17:4080–4092.
69. Waterham HR, Titorenko VI, Haima P, Cregg JM, Harder W, Veenhuis M. The *Hansenula polymorpha PER1* gene is essential for peroxisome biogenesis and encodes a peroxisomal matrix protein with both carboxy- and amino-terminal targeting signals. J Cell Biol 1994;127: 737–749.
70. Yaffe MP, Schatz G. Two nuclear mutations that block mitochondrial protein import in yeast. Proc Natl Acad Sci U S A 1984;81:4819–4823.
71. Schiestl RH, Gietz RD. High efficiency transformation of intact yeast cells using single stranded nucleic acids as a carrier. Curr Genet 1989;16:339–346.
72. Freitag M, Hickey PC, Raju NB, Selker EU, Read ND. GFP as a tool to analyze the organization, dynamics and function of nuclei and microtubules in *Neurospora crassa*. Fungal Genet Biol 2004;41: 897–910.